

1 Introduction

1.1 Phase Transitions and Nucleation

First-order phase transitions play an important role in science and nature as well as in many technical applications. Simple examples are condensation, evaporation, crystallization, and melting. These first-order phase transitions do not necessarily start right away at equilibrium: first, they need to overcome an energy barrier, which is the work of formation of a small embryo or nucleus of the new phase, which emerge from fluctuations within the old phase. This initiating process of most first-order phase transitions is called nucleation.

Apart from these simple, everyday examples, nucleation is vital in many other fields. In biophysics, the nucleation of bubbles in the DNA is essential for its replication and transcription.⁵ The crystallization of proteins is vital for the building of their structure and in the development of new drugs, and it is behind many diseases such as sickle-cell anemia or Alzheimer.⁶ A fundamental step in the replication of a virus is the self-assembly of its rigid shell from its proteins, which may be described by a nucleation mechanism.⁷ Bubble nucleation and crystallization are important processes in polymers.⁸ In microemulsions, we encounter micellar formation and liquid-liquid phase transitions, e.g. from a bicontinuous sponge to a micellar oil-in-water phase.⁹ The formations of black holes¹⁰ or volcano eruptions¹¹ are further examples involving nucleation.

One of the simplest examples to illustrate the mechanism of nucleation is the formation of a small liquid droplet in a supersaturated vapor. If we compress a vapor at constant temperature, the condensation will not commence at the saturation pressure, but above it: the vapor remains in a metastable state for some time until thermal fluctuations form a sufficiently large cluster or nucleus, which can grow on spontaneously.

⁵ Ares *et al.*, 2005.

⁶ Lyras *et al.*, 1997.

⁷ Zandi *et al.*, 2006.

⁸ Lansac and Tenbosch, 1991; Nagarajan and Myerson, 2001; Ki, Kang, and Kwak, 2004; Yamamoto and Sawada, 2005.

⁹ Kahlweit *et al.*, 1988; Sottmann and Strey, 2005.

¹⁰ Kapusta, 1984; Barrow, Copeland, and Liddle, 1992; Garriga and Vilenkin, 1993.

¹¹ Blander, 1979.

In this case, the barrier towards the condensation arises from the work needed to build the curved surface of a small liquid droplet in the vapor. The formation of clouds in the atmosphere, essentially the condensation of water vapor, is such an example.¹²

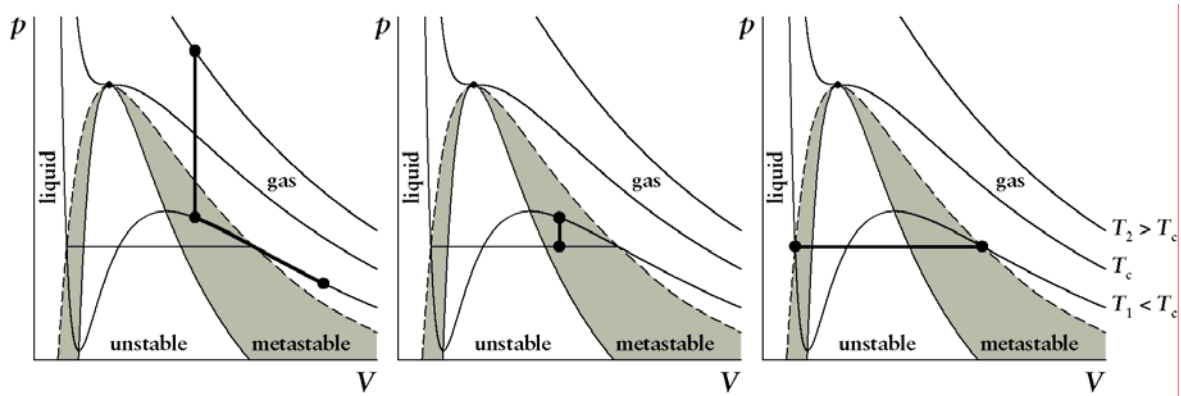


Figure 1.1: Pressure-volume phase diagrams of three isotherms of a van-der-Waals fluid above, below, and at the critical temperature T_c . From left to right: the vapor enters the metastable region by a compression or similarly via an expansion. The vapor pressure stays higher than the equilibrium pressure given by the Maxwell construction (horizontal line), until nucleation sets in. Finally, the two stable phases form out.

Figure 1.1 illustrates pressure-volume phase diagrams of a simple van-der-Waals fluid.¹³ The binodal (dashed line) separates the stable from the metastable region. When the fluid is in the metastable region (gray area), nucleation is the mechanism starting the phase transition. The spinodal (solid barrier to the gray area), in this case defined by the minima and maxima of the van-der-Waals loops, separates the metastable from the unstable region, where the fluid instantly undergoes a process called spinodal decomposition.

Broadly speaking, spinodal decomposition can be imagined as one large long-wavelength fluctuation of small amplitude that separates the two phases almost instantly and everywhere at the same time. Conversely, nucleation is by its very nature a stochastic process occurring randomly at unpredictable positions by the localized fluctuations of large amplitude.¹⁴ Metaphorically, nucleation behaves like popcorn: even though we know the corns will pop eventually and almost at a constant rate (i.e. a constant number of “pops per time and space”), we cannot predict exactly when and where an individual corn will pop.¹⁵ Figure 1.2 and Figure 1.3 illustrate the distinct differences of nucleation and spinodal decomposition by schematic density cuts

¹² See e.g. Laaksonen, Talanquer, and Oxtoby, 1995; Seinfeld and Pandis, 1998.

¹³ van der Waals, 1873.

¹⁴ See e.g. Debenedetti, 1996.

¹⁵ Admittedly, it is hard to imagine popcorn undergoing spinodal decomposition, even though it would considerably reduce queuing times in cinemas.

through a supersaturated vapor and the corresponding snapshots taken from a simulation of a two-dimensional Lennard-Jones (LJ) fluid.¹⁶

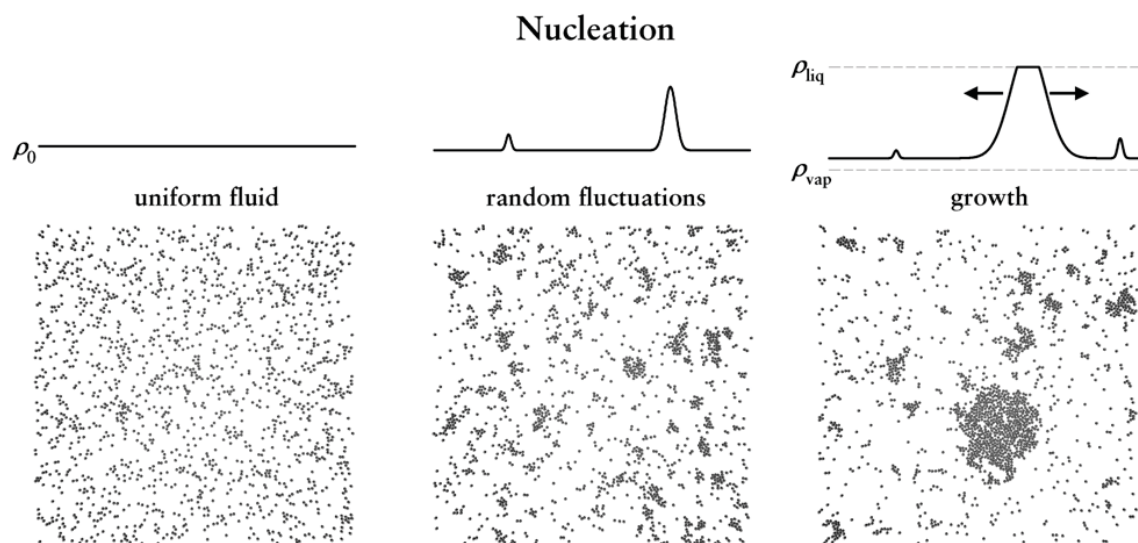


Figure 1.2: Schematic density cuts through a supersaturated vapor undergoing nucleation and corresponding screenshots of a simulation of a 2D Lennard-Jones proceeding in time from left to right for 20 ns. Nucleation occurs by random thermal fluctuations that slowly generate small aggregates of molecules, called clusters. When these clusters overcome a critical size, they can spontaneously grow towards the stable fluid phase.

In nucleation (Figure 1.2), only a few clusters form and continue growing and translating through the system. Spinodal decomposition (Figure 1.3) on the other hand clearly shows a wavelike decomposition resulting in interconnecting regions of high and low densities. Note that while the time span from left to right is about 20 ns for nucleation, spinodal decomposition already separated the two phases in less than 0.2 ns.

The resemblance of spinodal decomposition (middle snapshot in Figure 1.3) to a bi-continuous sponge phase of a microemulsion is remarkable.¹⁷ However, while the latter corresponds to a thermodynamically stable phase, the interconnected vapor and liquid-like regimes very quickly separate and eventually break up into individually growing cluster. Both the binodal and the spinodal coincide at the critical point. Therefore, the closer we get to the critical point of a system, the closer the stable, metastable and unstable states are to each other. Here, even small fluctuations are sufficient to change from one state to the other, which leads to a number of interesting critical phenomena, for example critical opalescence.¹⁸

¹⁶ Details on the 2D simulations can be found in the appendix.

¹⁷ Sottmann and Strey, 2005.

¹⁸ See e.g. Stanley, 1971.

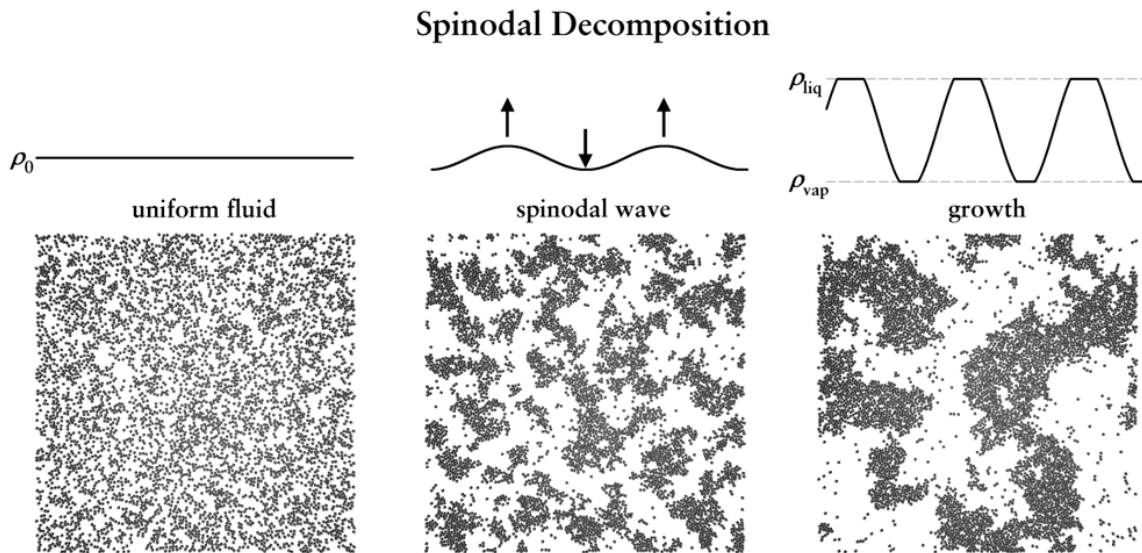


Figure 1.3: Schematic density cuts through a supersaturated vapor undergoing spinodal decomposition and corresponding screenshots of a 2D Lennard-Jones simulation, proceeding in time from left to right for only 0.2 ns. Spinodal decomposition manifests itself as a large continuous density fluctuation through the whole system. The local densities diverge towards the liquid or vapor density, respectively. This wavelike decomposition quickly results in interconnecting regions of high and low densities that eventually break up into large clusters.

A first-order phase transition, according to the definition of Ehrenfest,¹⁹ is characterized by a discontinuity in the first-order derivative with respect to the temperature of one thermodynamic quantity. Such a quantity could be the enthalpy H , the chemical potential, or the volume. We can easily picture what this means: when we heat up water in a pot on a stove, its temperature will rise up to the boiling point (100 °C at 1 bar). The temperature of the boiling water-vapor mixture stays constant even though we continue to transfer heat from the stove to the pot. As a result, the heat capacity $C_p = (\partial H/\partial T)_p$ appears to be infinite for some time,²⁰ which corresponds to a discontinuity in the enthalpy H .

After nucleation, a phase transition continues through growth and aging stages towards the full formation of the new phase, which finally is in thermodynamic equilibrium with the old phase, for example the final states in the right-hand diagram of Figure 1.1. These stages of first-order phase transitions are usually distinguishable by largely different time-scales. Nucleation, as the first stage, determines many important properties of the newly forming phase such as the number density and the size distribution of the nuclei. We need to understand the nucleation process in order to control these parameters in experiments or technical applications. For instance, the number

¹⁹ See e.g. Atkins, 1998.

²⁰ Naturally, in any real experiment the heat capacity would be very high, but finite. See e.g. Landau and Lifshitz, 1968.

and size of nucleating water droplets has an impact on the efficiency and lifetime of a steam turbine²¹ as well as the color and reflectivity of clouds, which influences the greenhouse effect.²² Semiconductors are known to be very sensitive to the number and size of defects on the silicon wafer.²³

In general, we have to distinguish homogeneous from heterogeneous nucleation. In heterogeneous nucleation, the phase transition begins on alien surfaces or particles present in the old phase. Dust particles for example or, more generally, atmospheric aerosol particles usually serve as heterogeneous nucleation centers for water condensation in the atmosphere. We can also induce heterogeneous nucleation in a one-component system by seeding nuclei of the new phase into the metastable phase. For instance, we can easily initiate crystallization of a saturated saline solution by adding just a few salt crystals to the solution. Heterogeneous nucleation usually has a smaller barrier towards the phase transition because it has to perform less surface work to build a nucleus of the new phase – in some cases growth can even commence without any noticeable nucleation step at all. Most phase transitions occurring in experiments or nature, such as cloud formation or crystallization, are heterogeneous. Nevertheless, the focus in nucleation research usually lies on the underlying homogeneous process: the formation of the new phase solely from fluctuations within the old phase of the pure substance. A complete understanding of homogeneous nucleation is a prerequisite towards a full description of all nucleation processes, including heterogeneous ones.

The most commonly used example of nucleation in experiment and theory is the vapor–liquid transition because it is well accessible by experiments and theoretical approaches, and of fundamental interest in atmospheric sciences. This work also focuses on homogeneous nucleation of the vapor-liquid transition.

1.2 Research on Vapor-Liquid Nucleation

First theoretical descriptions of vapor-liquid equilibrium can be found in works of Gibbs in the 19th century.²⁴ A first complete theory including the kinetics of vapor-liquid nucleation was presented by Becker and Döring in 1935, based on works of Volmer and Weber, and Farkas.²⁵ This so-called classical nucleation theory (CNT) is still the most widely used model for nucleation. Since then, numerous corrections and additions to CNT, as well as completely new theoretical approaches have been introduced with varying success since then, as will be discussed in Chapter 2. A review of

²¹ Bohn *et al.*, 2004.

²² Schwartz, 1996.

²³ Reboredo, Ferconi, and Pantelides, 1999.

²⁴ See completed works of Gibbs, Gibbs, 1961.

²⁵ Volmer and Weber, 1926; Farkas, 1927; Becker and Döring, 1935.

nucleation theory up to 1992 was given by Oxtoby.²⁶ In addition, excellent textbooks are available.²⁷

Many different experimental methods have been devised to study vapor-liquid nucleation. In terms of the nucleation rate J , which is the number of droplets forming per unit time and volume, these experiments cover an extraordinary range of more than 20 orders of magnitude.²⁸ Figure 1.4 is an overview of different methods and their respective measuring range.

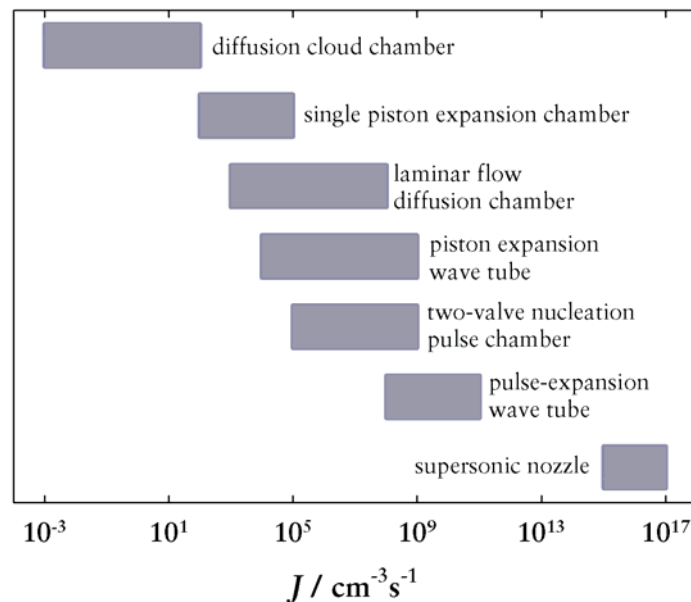


Figure 1.4: Different vapor-liquid nucleation experiments and their respective measuring window (details and references: see text).²⁹

On the low end, diffusion cloud chambers determine nucleation rates as low as $10^{-3} < J / \text{cm}^{-3} \text{s}^{-1} < 10^3$, while supersonic nozzles reach up to $10^{15} < J / \text{cm}^{-3} \text{s}^{-1} < 10^{17}$. The middle range of the measuring window is dominated by expansion chambers, such as the single-piston expansion chamber,³⁰ the piston expansion wave tube chamber,³¹ the two-valve nucleation pulse chamber (based on the two-piston expansion chamber),³² and the pulse-expansion wave tube.³³ An exception to the rule is the recent laminar

²⁶ Oxtoby, 1992.

²⁷ Abraham, 1974; Debenedetti, 1996; Kashchiev, 2000.

²⁸ For a review of nucleation experiments see Heist and He, 1994; Laaksonen, Talanquer, and Oxtoby, 1995.

²⁹ Figure according to Iland, 2004.

³⁰ Allard and Kassner, 1965.

³¹ Peters, 1982.

³² Wagner and Strey, 1984; Strey, Wagner, and Viisanen, 1994; Strey, Viisanen, and Wagner, 1995.

³³ Looijmans and vanDongen, 1997.

flow diffusion chamber.³⁴

The two-valve nucleation pulse chamber developed by Wagner and Strey is capable to determine isothermal nucleation rates and, consequently, the molecular content of the nucleus by making use of the so-called nucleation theorem, which will be discussed in section 2.4. This technique brought forth a number of studies on different substances, including the *n*-alcohols,³⁵ *n*-alkanes,³⁶ and state-of-art measurements of water nucleation.³⁷

Fladerer followed the success and reliability of this experimental setup and its highly reproducible results and devised a new cryogenic nucleation pulse chamber that uses the same experimental method.³⁸ Contrary to the two-valve chamber, the cryogenic chamber works at liquid nitrogen instead of room temperature, which enabled reproducible measurements of vapor-liquid nucleation of argon for the first time. Later, Iland was able to extend the range of accessible nucleation temperatures for argon and successfully measured the nucleation onset of nitrogen.³⁹ The experiments by Fladerer and Iland only determined the onset of nucleation (see Figure 1.5), i.e. the vapor pressure at which liquid droplets were detected for the first time as the growth rate of argon and nitrogen droplets turned out to be too fast to be decoupled from nucleation in the experiment. Still, the corresponding nucleation rate window of the cryogenic nucleation pulse chamber is similar to the window of the two-valve nucleation pulse chamber, which is determined by the detection method and known to lie in the range $10^5 < J / \text{cm}^{-3}\text{s}^{-1} < 10^9$. Based on this, Fladerer and Iland defined the nucleation rate in their experiments at $J = 10^{7 \pm 2} \text{cm}^{-3}\text{s}^{-1}$. Although this appears to be a crude measurement, the two orders of magnitude in error are small compared to the prediction of nucleation rates from CNT. It turns out that the theoretical prediction deviates by 16 to 26 orders of magnitude for argon and 10 to 20 orders of magnitude for nitrogen, depending on the temperature. This enormous disagreement is very surprising as most researchers assumed a very small discrepancy for a simple and almost ideally behaved substance such as argon. Thus, non-idealities of the investigated substance alone cannot account for the deviations of nucleation experiments.

Nevertheless, since the properties of argon can be successfully modeled by a simple Lennard-Jones potential, argon is the ideal substance to compare the accuracy or validity of more elaborate theories and computer simulations, which both require an accurate intermolecular potential. In the argon experiments, the initial temperature of the nucleation pulse chamber was fixed at the temperature of liquid nitrogen. This some-

³⁴ Lihavainen and Viisanen, 2001.

³⁵ Strey, Wagner, and Schmeling, 1986; Strey and Viisanen, 1993; Viisanen and Strey, 1994; Hrubý, Viisanen, and Strey, 1996; Wedekind, 2003; Iland *et al.*, 2004.

³⁶ Wagner and Strey, 1984; Wagner and Strey, 2001.

³⁷ Wölk and Strey, 2001; Wölk *et al.*, 2002.

³⁸ Fladerer, 2002; Fladerer and Strey, 2006.

³⁹ Iland, 2004.

what limits the flexibility of the temperature range, in which nucleation can be observed. Thus, deep expansions to very low temperatures in the range $42 \text{ K} < T / \text{K} < 58 \text{ K}$ were necessary to achieve a sufficiently high supersaturation. Figure 1.5 shows the onset vapor pressures of the argon experiments performed by Iland in a p - V phase diagram.⁴⁰

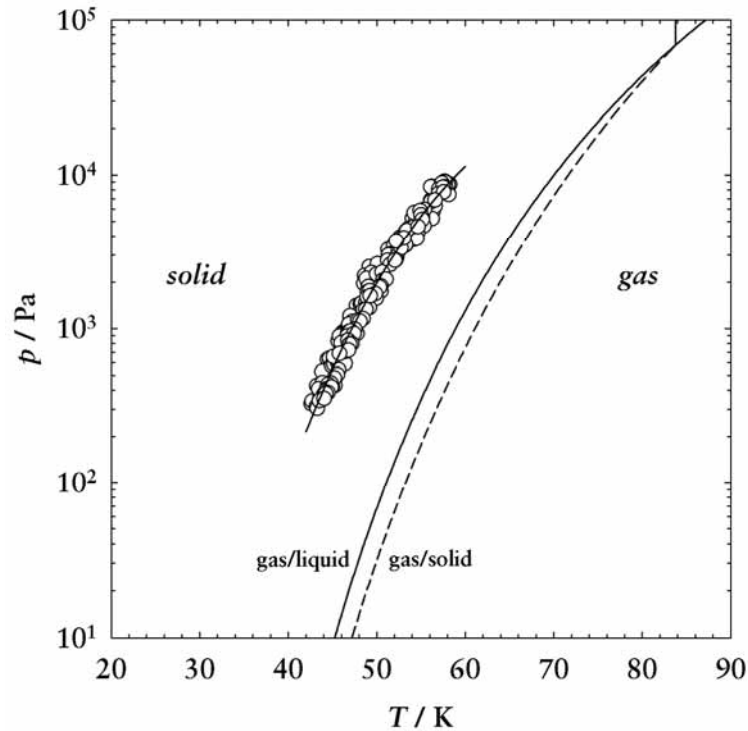


Figure 1.5: Onset vapor pressures of argon in a p - V phase diagram.⁴⁰ The solid line is the gas–liquid binodal, the dashed line the gas–solid binodal. All measurements are well below the triple point of argon (upper right corner) and deeply within the stable solid region of the bulk phase diagram.

The reported onset pressures are obviously deep within the stable solid region of the argon phase, while still being reported as onsets of a vapor-to-liquid nucleation. In fact, from the experimental data as well as from theoretical considerations, it is reasonable to assume that the vapor first condenses to liquid drops, which subsequently freeze.⁴¹ In this temperature range, computer simulations of nucleation have never been performed to date. The experimental results and huge deviations to nucleation theory therefore strongly motivated first simulations of argon nucleation in the same temperature range as the experiments.

The use of computers and in particular computer simulations as a means for civil scientific investigations began shortly after World War II. In 1953, Metropolis devel-

⁴⁰ Iland, 2004.

⁴¹ See discussion in section 7.1.

oped the “Monte-Carlo” (MC) method and performed the first simulations of a hard-sphere fluid in Los Alamos.⁴² The name “Monte-Carlo” is an innuendo to the stochastic nature of the method, much like gambling in a Casino in Monaco. Shortly afterwards, first simulations of a Lennard-Jones fluid were performed, allowing first reasonable comparisons of simulation and experimental results.⁴³ Around the same time, the method of molecular dynamical (MD) simulation was developed: Alder and Wainwright performed the first MD-simulations of hard spheres in 1957.⁴⁴ In MD, the classical equations of motion are solved numerically, thus tracking the system in time. Nowadays, computer simulations have become an indispensable research tool in many fields of natural sciences.⁴⁵

The simulation of nucleation is an extremely time-consuming task because nucleation is a rare event and often many particles have to be simulated. Consequently, direct simulations of nucleation were not feasible for a long time. To name just a few of many pioneering works in this field, Swope and Anderson simulated the formation of a crystal from a Lennard-Jones-fluid by introducing a preformed crystal into a supersaturated melt in 1990.⁴⁶ In 1998, ten Wolde and Frenkel presented extensive MC simulations of the condensation of a Lennard-Jones fluid, while shortly afterwards Yasuoka and Matsumoto performed large-scale MD simulations of the same transition.⁴⁷ MD simulations have the great advantage of gaining insights into the dynamics of the nucleation process, while MC simulations typically yield time-independent ensemble averages. Therefore, MD simulations were also employed in this work to gain further insights into the kinetics of nucleation.

In spite of the impact of nucleation on a huge variety of processes, many scientists who are not focused on nucleation as a research topic in itself naively assume that it is a problem, which has long been solved. This peculiarity might have to do with the fact that nucleation mainly is a “classical” problem in the sense that usually no quantum mechanics is necessary in the description of the process. Furthermore, a lot of attention has been devoted to the study of critical phenomena and universal scaling laws in the 20th century.⁴⁸ In this light, homogeneous nucleation or, specifically, the condensation of a one-component system far from the critical point may appear at first glance to be a comparatively trivial and solvable problem. Yet, the opposite is true: there is arguably no other discipline in contemporary science where deviations of several orders of magnitude between experiments and theory are still rather the rule than the excep-

⁴² Metropolis *et al.*, 1953.

⁴³ Wood and Parker, 1957.

⁴⁴ Alder and Wainwright, 1957; Alder and Wainwright, 1959.

⁴⁵ For an overview see e.g. Allen and Tildesley, 1989; Frenkel and Smit, 2002.

⁴⁶ Swope and Andersen, 1990.

⁴⁷ ten Wolde and Frenkel, 1998; Yasuoka and Matsumoto, 1998.

⁴⁸ See e.g. Stanley, 1971.